Cover Page

Universiteit Leiden

The handle http://hdl.handle.net/1887/21704 holds various files of this Leiden University dissertation

Author: Gupta, Vikas
Title: Multimodality cardiac image analysis for the assessment of coronary artery disease
Issue Date: 2013-09-11

4

A frequency domain approach to respiratory motion correction in cardiac MR stress perfusion sequences

This chapter was adapted from:

V. Gupta, M. van de Giessen, H. A. Kirişli, S. Kirschbaum, W. J. Niessen, and B. P. F. Lelieveldt. **Robust motion correction in the frequency domain of cardiac MR stress perfusion sequences**, *Medical Image Computing and Computer-Assisted Intervention - MICCAI*, Pages 667–674, 2012.

Abstract

First-pass myocardial perfusion MR (CMRP) imaging allows identification of hypo-perfused areas in the myocardium and therefore helps in early detection of coronary artery disease (CAD). However, its efficacy is often limited by respiratory motion artifacts, especially in images acquired under stress. These artifacts lead to unreliable estimates of perfusion linked parameters, such as relative up-slope and myocardial perfusion reserve index (MPRI). Although several methods exist to eliminate such artifacts in rest images, fewer motion correction methods have been reported for stress images. To this end, we propose a novel and robust motion correction method that suppresses motion artifacts in the frequency domain and allows fast and near-automated computation of MPRI values. The method was validated for registration accuracy and perfusion parameters using 120 sequences including both rest and stress images and is compared to state-of-the-art registration methods based on independent component analysis and pairwise normalized cross-correlation. In terms of registration accuracy, the proposed method outperformed the other methods by a significant margin. Of particular interest were the reduction of large displacements to sub-pixel motion after registration with the proposed method. Additionally, its suitability to clinical use was shown by strong agreements with the gold standard perfusion parameters. Conclusively, the robustness and accuracy of the proposed method demonstrate its potential for a near-automated quantitative analyses of not only rest, but also the more challenging stress MR perfusion sequences in a routine clinical setting.

ASSESSMENT of myocardial perfusion with magnetic resonance (MR) imaging provides valuable insights into the extent and location of coronary artery diseases (CADs). Typically, cardiac MR perfusion (CMRP) images of 3-5 short-axis slices of the heart are acquired about 60 seconds after the injection of contrast. To improve differentiation of normal from hypo-perfused tissues, images are acquired at rest and during stress using a pharmacological vasodilator such as adenosine or dipyridamole. In addition, breath-holding and electrocardiogram (ECG) based triggering are used to ensure that the motion of the heart is effectively frozen during the acquisition of images over multiple cardiac cycles (Figure 4.1). These multiple frames or images for a given slice position form one image sequence and each acquisition may result in 3-5 sequences based on the number of slice levels. Typically, the visual analysis of a CMRP image sequence in cine-loop suffices for the identification of distinct hypo-perfused myocardial regions. Nevertheless, subtle differences that might be required for follow-up examinations and therapeutic planning, may elude even an experienced observer. Furthermore, a visual analysis is prone to inter- and intra-observer variability. It is therefore of interest to supplement subjective qualitative analysis with an objective and quantitative assessment of myocardial perfusion. Relevant quantitative perfusion parameters include relative up-slope, myocardial perfusion reserve index (MPRI), etc. Among them, MPRI is considered the most significant as it indicates the ischemic burden of the myocardium [6, 112]. For the computation of these parameters, time-intensity curves (TICs) (Figure 4.3) are required, which can be obtained by sampling myocardial intensities in all the frames of a CMRP image sequence. The relative up-slope refers to the ratio of the maximum up-slopes of TICs derived from the myocardium and blood pool during the first pass of contrast agent through the heart. In contrast to the relative up-slope which is estimated separately for rest and stress studies, the MPRI is defined as the ratio of hyperemic (during stress) and basal (at rest) myocardial blood flow. It is often computed as the ratio of relative up-slopes at stress and rest[6, 112]. To reliably estimate these parameters, it is essential that the myocardial intensities are sampled from the same region of interest in all the frames of a sequence. However, this constraint cannot be satisfied in many patients (especially those with CAD) because a prolonged single breath hold frequently results in sudden respiration during the image acquisition, and as a consequence, to displacement and/or deformation of the heart[94, 147, 216]. Such motion artifacts lead to distorted TICs that provide unreliable estimates of perfusion linked parameters. Due to the vasodilatory effects of pharmacological agents, these artifacts are often more pronounced in images acquired under stress.

Elimination of respiratory motion artifacts in CMRP images, therefore, poses two main challenges: (a) irregularity of frame displacements in a sequence, and (b) dynamic contrast variations caused by the passage of contrast agent through the heart. Several semi- and fully-automatic registration methods have been proposed to overcome these challenges, predominantly in sequences at rest. An in-depth overview of these algorithms is given in [94]. Most of these methods include intensity or model based registration wherein the motion correction is performed by aligning the images in a sequence either to a reference frame [3, 30, 36, 56, 68, 84, 92, 116, 232, 267] or to their neighboring frames[268]. Generally, this alignment is achieved using a similarity measure based on squared intensity differences [30], normalized cross-correlation[92], mutual information[19, 36], and gradient information[231]. As most of these methods involve pairwise image alignments, they tend to suffer from the propagation of residual

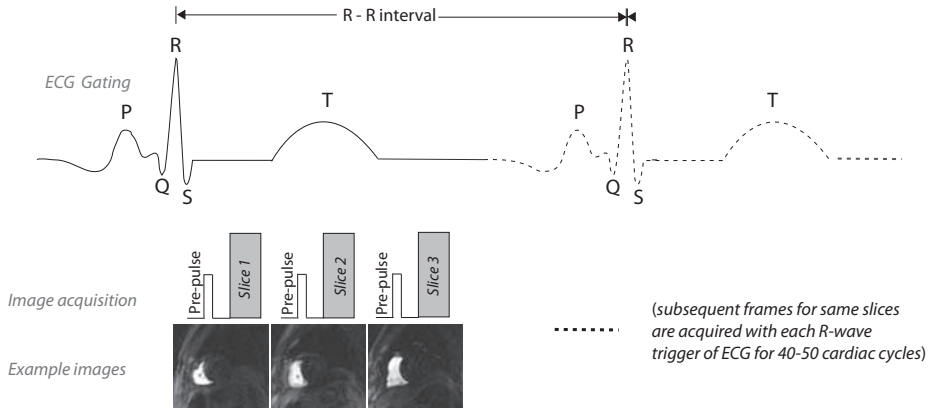

Figure 4.1: This schematic of a typical CMRP image acquisition shows how the cardiac contraction is frozen by synchronizing the image acquisition to the cardiac cycle using ECG gating[94].

registration errors. The error propagation resulting from the selection of a single reference image was reduced by two recently proposed approaches[93, 154]. These methods took into account the characteristic temporal contrast variation in the perfusion sequence using independent component analysis (ICA). The component images and their corresponding weights obtained from ICA were used to generate a distinct reference image for each frame of the sequence. The dependence on initial component estimation using ICA, however, may lead to unreliable registration in the presence of flickering intensity changes and large motion artifacts, present especially in stress images. A similar approach was used in [263], but its applicability was limited by an inherent assumption of quasi-periodicity in free breathing sequences. The modified version of this ICA[154] based approach was recently proposed in [264], where a new labeling scheme, based on discrete wavelet analysis, was to used to perform an optimal separation and selection of independent components. However, this method was designed for free breathing sequences and its validation was performed using only a few simulated breath-hold sequences. As such, the suitability of this method on real breath-hold sequences remains unconfirmed.

Although most of the existing strategies strategies perform satisfactorily for rest image sequences, their efficacy on stress images from patients suspected of CAD has not been proven yet. Due to the physiological effects of pharmacological stress agents on patients with CAD, breathing motion may be considerably larger in stress images than in the rest images. In pilot experiments with both types, we found that both types of existing registration strategies, i.e., pairwise and initial global component estimation[93, 154], often result in an unreliable registration of stress image sequences.

This paper presents a novel frequency domain approach to eliminate motion artifacts present especially in stress CMRP image sequences. The proposed method exploits the fact that motion artifacts in a CMRP image sequence manifest themselves primarily as distortions in the TIC (Figure 4.2(b)) and as undesired high frequency content in TIC's frequency spectrum (Figure 4.2(d)). We perform an iterative minimization of the high

frequency content present in TIC's frequency spectrum by concurrently aligning the frames in the CMRP image sequence thereby avoiding the problem of residual error propagation. The proposed frequency domain approach makes very few assumptions on the expected scan data (e.g., free breathing or breath-hold) and is aimed to be robust against both (a) large and irregular breathing movement of the patient, and (b) flickering intensity variations.

Parts of this work have been presented at MICCAI[95]. Compared to that work, we have significantly extended the method descriptions, and presented a more comprehensive validation on a larger pool of data and more clinical parameters. In addition, a comparison to previously published motion correction methods has also been included.

In section 4.1, we present the proposed method along with the formulations and follow it with the sections describing data and experiments. Subsequently, results of the validation on data comprising 120 rest and stress sequences from 20 patients are presented. Finally, a discussion on the results and the future work follows in the concluding section.

4.1 Method

4.1.1 Registration

As shown in Figure 4.2, sudden intensity changes caused by motion artifacts show up as undesired high frequency content in TICs. Using a high pass filter this content can be separated from the frequencies present in a sequence without motion artifacts. We propose to model the high frequency content as a cost function of the translations of all the frames in the sequence. Minimizing this cost function concurrently over all frames should then remove the motion artifacts.

Let us denote the intensity profile of a pixel at coordinates x, y in an input image sequence, I, with N frames as $I_{x,y}(t)$. The frequency content of this time-intensity curve is then given by the discrete Fourier transform (DFT):

$$\hat{I}_{x,y}(\omega) = \mathscr{F}[I_{x,y}(t)] = \sum_{t=0}^{N-1} I_{x,y}(t) e^{-j2\pi\omega t/N} \tag{4.1}$$

where t and ω refer to time (in this work, frame number) and frequency, respectively.

We define a high pass filter, $H(\omega)$, that passes the high frequency components which we assume are present due to motion artifacts. Because the filtered signal in the frequency domain is complex, the energy spectral density of the signal is used to form the cost for the intensity profile at $I_{x,y}$:

$$C_{x,y} = \frac{1}{2\pi} \sum_{\omega} \left(H(\omega)\hat{I}_{x,y}(\omega)\right)\left(H(\omega)\hat{I}_{x,y}(\omega)\right)^* \tag{4.2}$$

where * denotes the complex conjugate. The total cost within a region of interest Ω is then given by:

$$C_{total} = \sum_{(x,y)\in\Omega} C_{x,y} \tag{4.3}$$

Using shifts, $Sx(t)$ and $Sy(t)$ to minimize C_{total}, for $t = 1, 2, 3, ..., N$, we can obtain the derivative of the total cost with respect to the shifts in x and y directions, respectively,

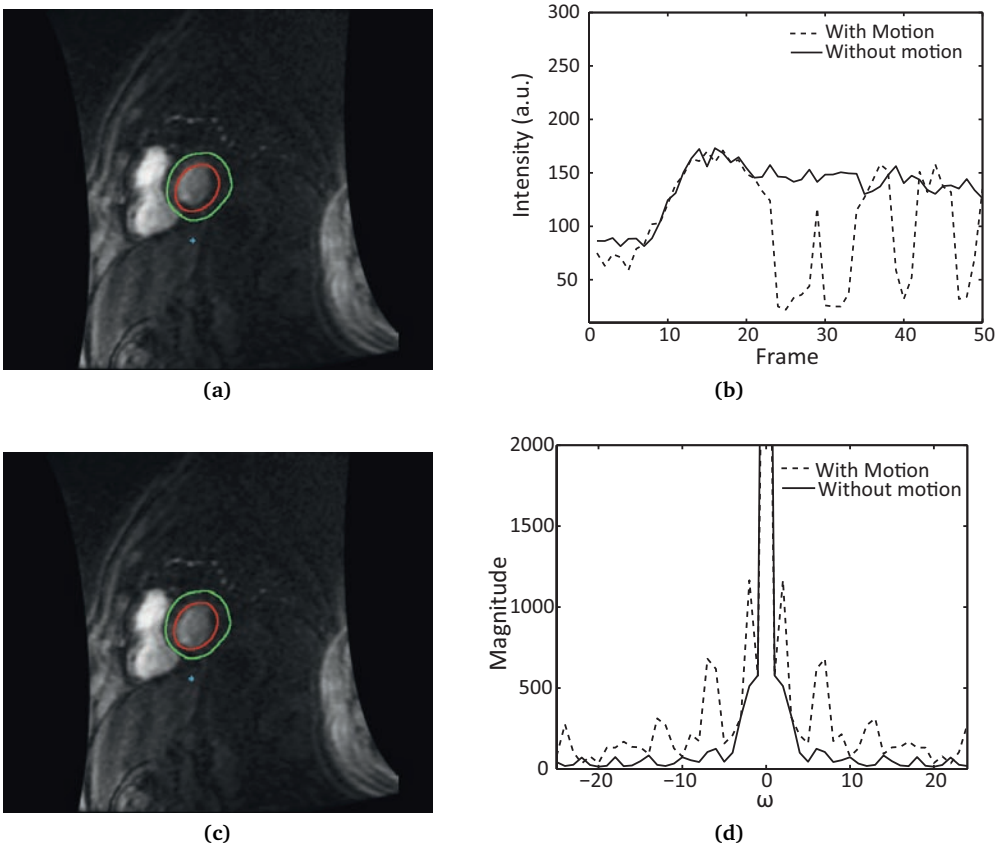

Figure 4.2: Typical frames of cardiac sequences (a) with motion and (c) without motion. The frames are annotated with epi- and endocardial contours. + indicates the RV insertion point.(b) Example time-intensity curves in the time domain and (d) in the frequency domain. The motion artifacts visible in the time domain show up as additional high-frequency content in the frequency domain.

from equation 4.3:

$$\begin{aligned} \frac{\partial C_{total}}{\partial Sx(t)} &= \frac{\partial}{\partial Sx(t)} \sum_{\Omega} C_{x,y} \\ &= \sum_{\Omega} \frac{\partial C_{x,y}}{\partial I_{x,y}(t)} \frac{\partial I_{x,y}(t)}{\partial Sx(t)} . \end{aligned} \tag{4.4}$$

$$\frac{\partial C_{total}}{\partial Sy(t)} = \frac{\partial}{\partial Sy(t)} \sum_{\Omega} C_{x,y} = \sum_{\Omega} \frac{\partial C_{x,y}}{\partial I_{x,y}(t)} \frac{\partial I_{x,y}(t)}{\partial Sy(t)} . \quad (4.5)$$

Algorithm 1: Motion correction algorithm

Data: An image sequence, I with N frames
Result: Optimal shifts, S (in x and y directions)
Initialize:;
S with zeros;
a mask encompassing only the LV and the RV;
$tolerance$;
$maxiter$;
begin
  while *not converged* **do**
    shift I by S;
    get time-intensity curves from pixels within the mask;
    compute the discrete Fourier transform (DFT) of each curve;
    compute cost for each curve using DFT;
    $F(Sk) \leftarrow$ sum of all costs for a shift S_k, where k is the iteration count;
    $G_k \leftarrow \bigtriangledown F(S_k)$;
    for $k = 0$ *to* $maxiter$ **do**
      $\alpha_k = \text{argmin } \phi(\alpha) = F(S_k - \alpha G k)$;
      $S_{k+1} = S_k - \alpha_k G_k$;
    end
    if $\| G_{k+1} \| \leq tolerance$ **then**
      converged ;
    end
  end
end

The computational overhead associated with the equations defined earlier can be reduced significantly by employing Vandermonde matrices, F, to compute the DFT, and vectors, $\mathbf{h}_\omega$ and $\mathbf{i}_{x,y}$, for the filter, $H(\omega)$, and time-intensity profile, $I_{x,y}(t)$, respectively. Consequently, $C_{x,y}$ can be evaluated inexpensively as:

$$C_{x,y} = \mathbf{i}_{x,y}^T F^* \mathbf{h}_\omega^* \mathbf{h}_\omega F \mathbf{i}_{x,y} \equiv \mathbf{i}_{x,y}^T W \mathbf{i}_{x,y} \quad (4.6)$$

where W is the same for each intensity profile, as it only depends on the number of frames. Each intensity value in $\mathbf{i}_{x,y}$ can be considered as a function of the transformation of the respective slice. For translations, $Sx(t)$ and $Sy(t)$ for frame, t, in the x and y directions, respectively, the gradient of the cost to these translations is given by:

$$\frac{\partial C_{x,y}}{\partial Sx(t)} = \frac{\partial C_{x,y}}{\partial \mathbf{i}_{x,y}} \frac{\partial \mathbf{i}_{x,y}}{\partial Sx(t)} = 2\mathbf{i}_{x,y}^T W \frac{\partial \mathbf{i}_{x,y}}{\partial Sx(t)} \quad (4.7)$$

where $\frac{\partial \mathbf{i}_{x,y}}{\partial Sx(t)}$ is the negative image intensity derivative in the x direction. A similar equation holds for the y direction.

Using a constant high-pass filter, $H(\omega)$, that blocks the undesired frequencies present in TICs distorted by motion artifacts, the complete motion correction procedure consists of two steps:

a. Automatically select the region of interest(ROI), Ω, containing the left and right ventricles.

b. Minimize (4.3) using a gradient-descent algorithm (Algorithm 1).

To avoid the trivial solution of moving all high frequency content out of the ROI, Ω, the sums of all translations in the x direction and all translations in the y direction are kept at 0. The important steps of the proposed method are summarized in Algorithm 1.

The proposed registration algorithm was implemented using a coarse to fine scheme so that the combinatorial complexity of the possible matches between a large number of small local patterns is avoided. This multi-resolution scheme not only allows computationally efficient processing of coarse transformation from low resolution images, but also decouples misalignments on finer scales from each other by limiting them to small and non-overlapping areas. In addition, this multi-resolution scheme is also suitable for parallel processing in the future.

4.1.2 Automatic ROI selection

Ideally, the CMRP images should present a signal intensity variation only in the heart. As the other organs surrounding the heart (e.g., lungs, liver) in CMRP images might interfere with the registration process of the heart, it is important to restrict the ROI to only the left ventricle (LV) and the right ventricle (RV). Being the major cavities of blood, the RV and the LV chambers display the maximum signal intensities during the first pass of contrast agent. We therefore adopted a maximum intensity projection based strategy to select an ROI. Based on the assumption that the heart lies approximately at the center of the field of view during the acquisition, following steps describe the automatic selection of an ROI in the proposed method:

a. Define a circular mask with radius R and center C is for an image sequence where the central pixel in each image serves as C; R is selected empirically. This mask serves to eliminate interference from the other organs surrounding the heart.

b. Compute the maximum intensity projection image, I_{mip} from the masked sequence obtained in last step.

c. Apply soft thresholding on I_{mip} to retain only the maximum intensity regions, viz., the RV and the LV. Soft thresholding allows the less intense regions such as epicardial boundaries to be also included within the ROI.

d. Compute the centroid of the thresholded image and assign it as the new center for the circular mask defined earlier.

4.2 Data

A dataset comprising 120 CMRP sequences from 20 patients with suspected CAD and normal left ventricular ejection fraction was used to validate the proposed method. All the images were acquired at Erasmus MC, University Medical Center Rotterdam, using a

1.5 Tesla MRI scanner (Signa CV/i, GE Medical Systems, Milwaukee, Wisconsin, USA) and a cardiac eight-element phased-array receiver coil placed over the thorax. The acquisition was performed using a steady-state free precession technique (FIESTA) and with Gd-DTPA (Magnevist, Schering, Germany) as the contrast agent. The temporal resolution per slice of 120 ms allowed imaging of 3-6 slices per R-R interval. Stress images were acquired 15 minutes after the acquisition of rest images using adenosine as the vasodilator. Both rest and stress images were acquired using the same pulse sequence and orientations. This study protocol was approved by the Ethics Committee of the Erasmus MC and a written informed consent was given by all the participating patients[124]. The selection of validation data was based on the criteria that each patient study must have: (a) sequences representing at least 3 slices with each of these three sequences consisting of equal number of frames, (b) sequences with sufficient number of frames depicting at least the first pass of the contrast agent, and (c) equal number of slices for both rest and stress studies. These criteria were used to ensure the consistency of image data for the comparison of different patient studies based on residual motion and perfusion parameters. As a result, each data set consisted of three slices (basal, mid-ventricular, and apical) of both a rest and a stress sequence of approximately 40-50 frames.

4.3 Experimental setup

The proposed method was validated on the basis of registration accuracy and clinically relevant perfusion parameters. For comparison purposes, the data were also analyzed with two previously published motion correction implementations by Milles et al.[154] based on ICA, and by Guizar et al. (single-step DFT algorithm in [91]), which is based on Normalized Cross-Correlation (NCC). The original implementations were used for performance benchmarking of the proposed FT-based registration. The selection of these two methods was motivated by the facts that cross-correlation based strategies have been one of the earliest and most widely used registration strategies[276], while ICA based methods have been shown to outperform the other existing methods[93, 154, 263, 264]. The validation was performed on data described in section 4.2. To perform an unbiased comparison, the NCC[91] based implementation was adapted to include the ROI selection identical to the proposed method. All rest and stress sequences were registered using the proposed method (FT), ICA based algorithm[154] and NCC based motion correction[91]. The NCC based registration follows the approach similar to the cascading pairwise registration adopted by [37] and [92] where an image acquired at time, t +1, was registered to the one acquired at time, t, using cross–correlation as the similarity measure.

4.3.1 Ground truth

The ground truth for the following experiments was obtained by delineating myocardium in each frame of all the unregistered perfusion sequences. The myocardial delineations in each frame of a sequence required the tracing of endo- and epicardial contours under a constraint that during translation intra-contour distance remains constant. This follows the underlying assumption that myocardial thickness remains constant over a given sequence thanks to the ECG gated image acquisition. The set of contours thus obtained serves as the ground truth for the validation of different methods and are henceforth referred to as ground truth contours. Similarly, the perfusion parameters computed using these contours are also referred to as ground truth parameters.

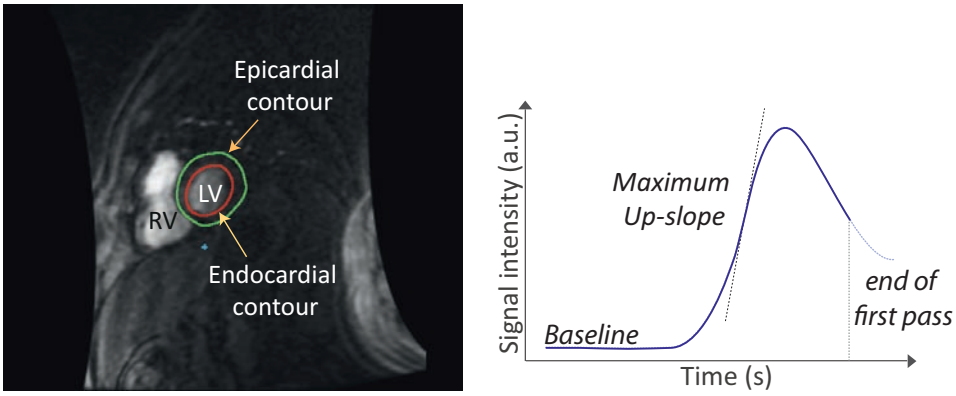

(a) A typical CMRP image **(b)** A TIC

Figure 4.3: An example of time intensity curve (TIC) and up-slope estimation

4.3.2 Validation experiments

4.3.2.1 Residual motion

Let the centroid of each frame in an image sequence, I, be denoted by $C(t)$, where $t = 1,2,...N$ and N represents the total number of frames in the sequence. Then the average displacement or residual motion, D, for the sequence, $I(t)$, can be computed by using the following equation:

$$D = \frac{1}{N}\sum_{t=1}^{N} C(t) - \bar{C}, \tag{4.8}$$

where $\bar{C}$ represents the mean centroid location. The residual motion, D, was computed for all the rest and stress sequences before and after registration with FT, ICA[154] and NCC[91] methods. The differences in the centroids of LV myocardial contours were used for the residual motion based validation under the constraints that the shape and the size of contours remain constant for each frame of the given sequence[92, 154]. This is in accordance to the underlying principle of CMRP image analysis that the heart must remain frozen during acquisition and signal intensities must be sampled from the same region in all the frames corresponding to each slice position.

4.3.2.2 Perfusion parameters

Ideally, the registered datasets should have no residual motion. Therefore, the perfusion parameters were computed by selecting only one pair of endo- and epicardial manual contours for each sequence and propagating it to all the frames. This resulted in 3 sets of test contours (one each for FT, ICA[154], and NCC[91]) that were used to sample myocardial intensities in the respective data sets. Thus performed intensity sampling led to TICs (Figure 4.3) that were used to compute various semi-quantitative perfusion parameters. We selected two such parameters: relative up-slope and MPRI, which are widely accepted as reliable perfusion indices[8, 112].

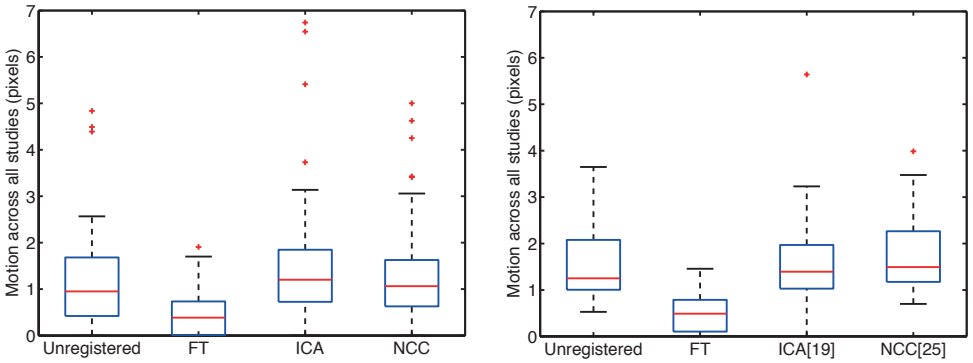

(a) Rest **(b)** Stress

Figure 4.4: Box plots for comparison of different methods based on residual motion in all the rest and stress sequences (Average pixel size 1.52 ± 0.05 mm isotropic)

To determine whether the perfusion parameters obtained from ground truth contours differ significantly from those obtained using contours drawn on registered images (FT), a paired samples t-test was performed at 95% significance level.

4.3.3 Implementation Details

A PC with Intel® Xeon® CPU at 3.3 GHz and 6 GB RAM was used for the execution of the implemented method. The implementation of both the proposed method and the validation experiments was done using Matlab® R2011b[2].

4.4 Results

4.4.1 Residual motion

The mean motion values in the unregistered, ICA[154] registered , and NCC[91] registered stress/rest images were 2.31/1.78, 2.36/2.23, and 2.71/2.02 mm, respectively. However, the motion in stress and rest images registered using the proposed FT method was reduced to 0.74 and 0.69 mm, respectively. This amounts to a motion reduction of 68% for stress and 61% for rest images across the whole population.

To investigate the degree of dispersion and skewness of the residual motion across all studies in different slices, box plots are shown in Figure 4.4. The box plots of FT registered datasets show lower medians, lower 25% and 75% quartiles, and comparatively less outliers compared to those in unregistered data sets.

The plots for absolute LV motion in rest and stress sequences, shown in Figure 4.5, indicate the correlation of the residual motion in unregistered sequence to the residual motion in sequences registered with different methods. A line segment with 45° slope is included in each of these plots to illustrate the effect of different registration methods- a marker below the segment shows reduction in original motion while its presence above the segment indicates the introduction of additional motion by the corresponding method.

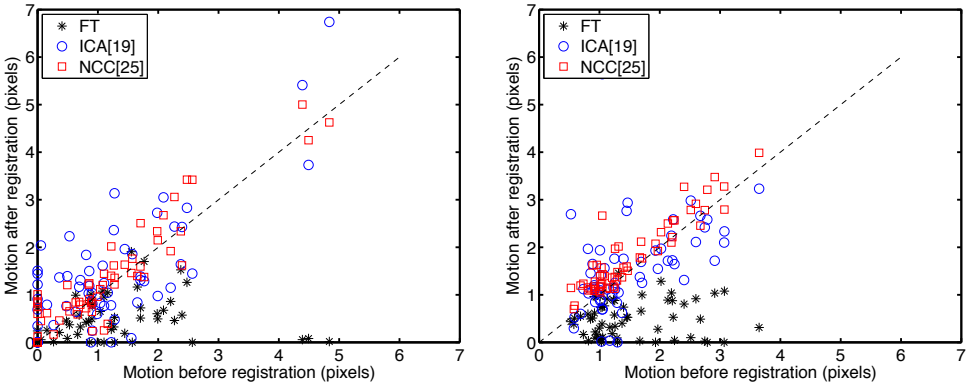

(a) Rest **(b)** Stress

Figure 4.5: Correlation plots for residual motion before and after registration with different methods in both rest and stress studies.

4.4.2 Perfusion parameters

The perfusion parameters were computed using the method described in section 4.3.2.2. We show an example of TICs obtained from unregistered and registered sequences in Figure 4.6. The corresponding frequency spectra are depicted in the second row of the same figure.

Figures 4.7(a) and (b) depict the correlation plots for relative up-slopes estimated after motion correction using the proposed method and compared to the up-slopes based on the contours annotated by the expert for stress and rest studies, respectively. The MPRI computed as the ratio of relative up-slopes at stress and rest is displayed in Figure 4.7(c). In addition, results of the regression analyses are also presented in the respective correlation plots. A further analysis of MPRIs is presented for all the sequences in Figure 4.8 which shows a comparison of MPRIs obtained from ground truth and FT registered sequences. The computation of MPRI relies on the relative up-slopes and the results of the paired samples t-test showed that the differences between relative up-slopes obtained using ground truth and FT contours were statistically insignificant ($p >> 0.05$, under the null hypothesis that the differences are insignificant). However, the relative up-slope estimates after ICA[154] and NCC[91] based motion correction were found to be significantly different ($p < 0.05$).

4.4.3 Computation time

Our experiments show that sequences of 40-50 frames can be automatically registered in 20 seconds compared to approximately 10 minutes required for manual annotation.

4.5 Discussion

We presented a novel frequency domain approach to motion correction in first-pass myocardial perfusion MR image sequences. By minimizing motion artifacts in the frequency domain using a high-pass filter, the motion correction problem became a

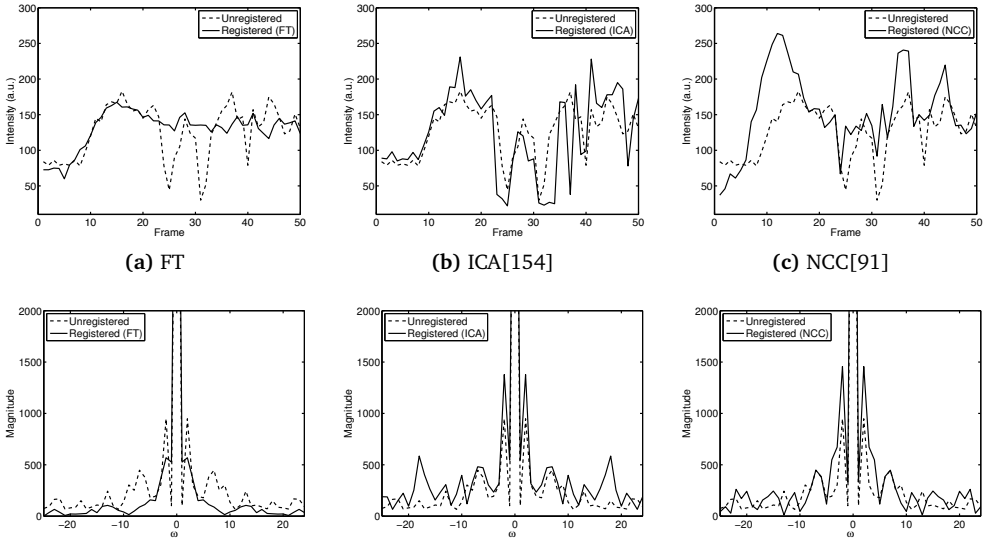

(a) FT **(b)** ICA[154] **(c)** NCC[91]

(d) FT **(e)** ICA[154] **(f)** NCC[91]

Figure 4.6: The first row depicts TICs obtained from a sequence before registration and after registration with FT, ICA[154], and NCC[91] based methods and the second row shows the corresponding frequency spectra.

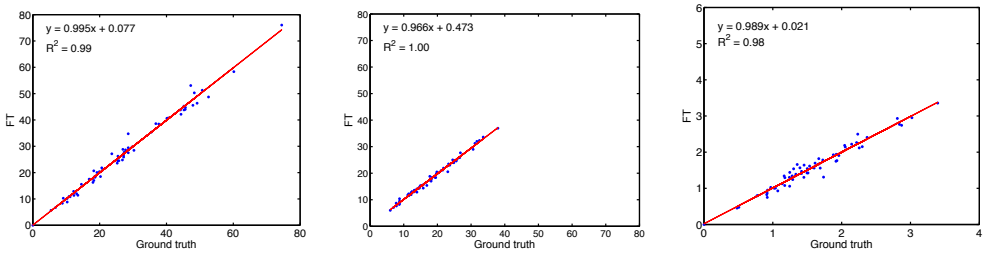

(a) Relative Up-slope (Stress) **(b)** Relative Up-slope (Rest) **(c)** MPRI (Up-slope$_{Stress}$/Up-slope$_{Rest}$)

Figure 4.7: Regression analysis of relative up-slopes and MPRIs obtained with ground truth and FT registered contours. The analysis is performed for both, stress and rest relative up-slopes.

simple quadratic function of time-intensity profiles that can be solved efficiently (Equation 4.2). The validation results described in section 4.4 show that the proposed method compares favorably with the existing registration methods[91, 154] based on both residual motion and perfusion parameters. A detailed discussion of the results with respect to the validation experiments and their clinical significance is provided in the following

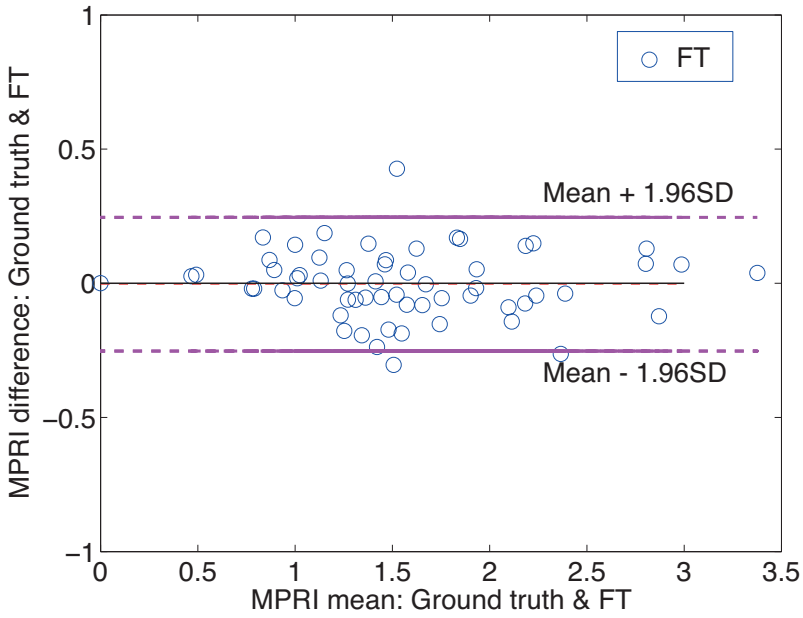

Figure 4.8: Bland Altman plot for Myocardial perfusion reserve index (MPRI) computed for the whole cohort: the plot shows a comparison of ground truth MPRIs with those computed from images registered using the proposed method (FT).

subsections.

4.5.1 Residual motion

As depicted in Figure 4.4, the residual motion results for the proposed method show an improvement over the current techniques both in terms of accuracy and robustness. The FT algorithm is apparently robust against rapidly varying intensities as indicated by the sub-pixel mean values in Figure 4.4. It can also be observed from Figure 4.5 that motion in FT registered sequences remains low despite the presence of large motion in original unregistered sequences. For the ICA[154] and NCC[91] implementations, the residual errors increase with increasing pre-registration motion (Figure 4.5).

The relatively bad performance of the ICA[154] based motion correction, especially in the stress sequences, can be attributed to the incorrect identification of the components on which its correction algorithm relies. These components mainly captured motion artifacts instead of time-intensity perfusion information and thus lead to (a) the incorrect mask selection, and (b) inaccurate reference images. Both of these factors hamper registration. An example of the correct and incorrect component labeling in ICA[154] based method is shown in Figure 4.9. We observed that the errors in labeling were mainly due to flickering intensity variations between consecutive frames. These intensity variations were also responsible for the relatively bad performance of the NCC[91] based registration, wherein the presence of secondary correlation maxima often makes it difficult to select the actual maximum. Furthermore, the determination of the maximum correlation position was

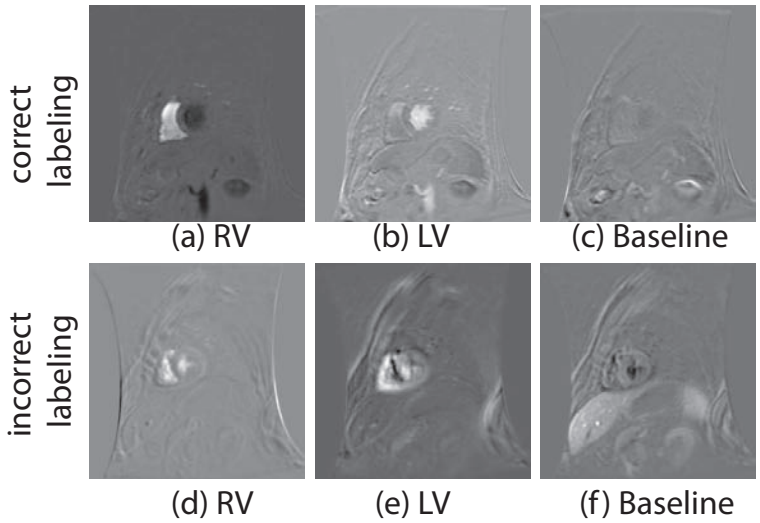

Figure 4.9: The component images obtained using the ICA[154] based registration: the first row shows an example of component images as a result of correct labeling of independent components, and the second row shows the corresponding images as a result of incorrect labeling. The reference image identification in ICA[154] based method relies on correct labeling of component images, the failure to do so results in sub-optimal registration.

unreliable due to the presence of a broad cross-correlation peak [276].

4.5.2 Perfusion parameters

A reliable computation of perfusion parameters requires undistorted TICs that show an absence of high frequency content in their Fourier spectra. To this end, Figure 4.6 shows the TICs obtained from a stress sequence before and after registration with FT, ICA[154], and NCC[91] based methods. As the computation of relative up-slopes is constrained specifically to the first pass, the segment of TICs corresponding to first 20 frames (in this example) are most significant and an analysis of these segments indicates that the maximum up-slopes will be overestimated for ICA[154] and NCC[91] registered datasets. The distortions in their TICs are reflected as high frequencies in the frequency spectra for the respective TICs. In comparison, high frequencies are subdued in the frequency spectrum from the sequence registered using the FT based method. This shows that the proposed algorithm is inherently robust to time-shifts in the acquisition.

Both, relative up-slopes and the MPRI values, are used in clinics to estimate the degree and extent of myocardial ischemia. The MPRI, being analogous to coronary flow reserve in the catheterization laboratory, can help in determining the functional significance of a coronary artery stenosis [128]. The results on relative up-slope and MPRI differences in Figures 4.7 and 4.8, respectively, provide an indication of the suitability of the proposed method in a clinical setting. The regression analyses between relative up-slopes obtained from the ground truth and the proposed method for both the stress and rest studies indicate a high degree of correlation (R^2 = 0.99 and 1, respectively)

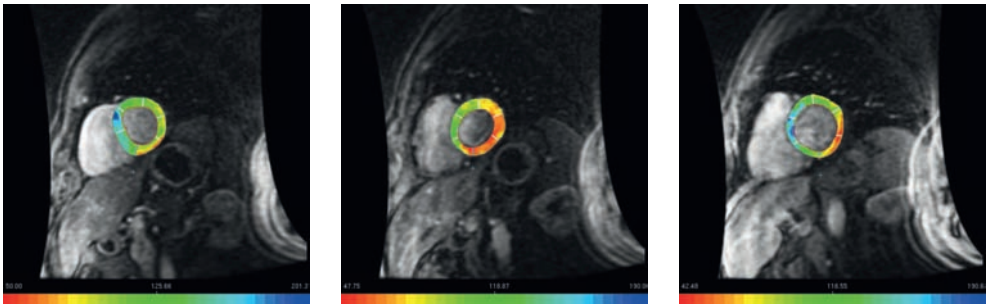

(a) Apical(Ground truth) **(b)** Mid-ventricular(Ground truth) **(c)** Basal(Ground truth)

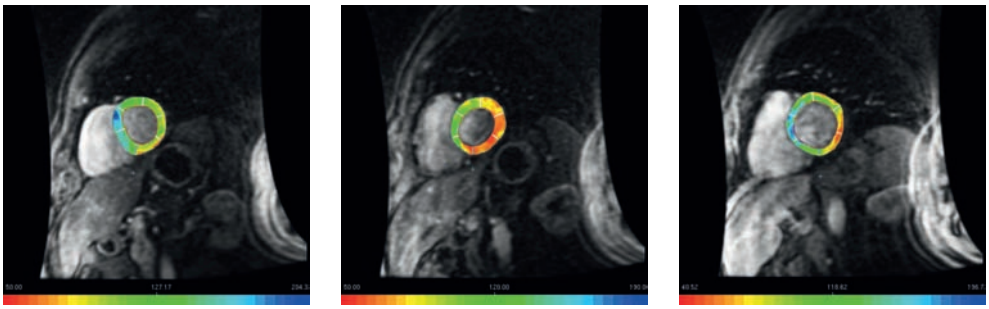

(d) Apical(FT) **(e)** Mid-ventricular(FT) **(f)** Basal(FT)

Figure 4.10: Mean myocardial signal intensities in apical, mid-ventricular and basal slices derived from the ground truth and FT contours for a CMRP sequence. The regions of hypo and normal perfusion in the myocardium are same in both the cases.

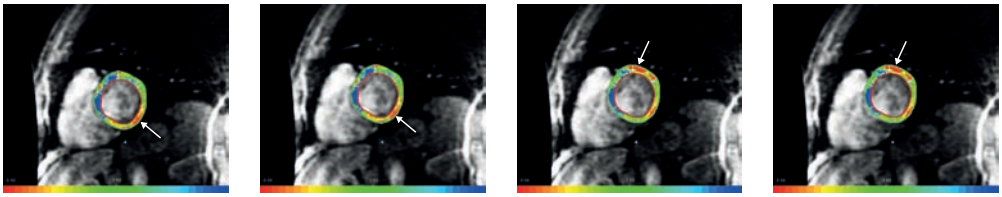

(a) Ground truth **(b)** FT **(c)** ICA[154] **(d)** NCC[91]

Figure 4.11: Myocardial blood flow estimates for basal slice showing the similarities and differences between the ground truth sequence and sequences obtained using FT, ICA[154] and NCC[91] based registration methods. The image corresponding to the proposed method (FT) shows similarities with the ground truth image i.e., the reduction of blood flow in inferolateral segment (arrow). However, the images corresponding to ICA[154] and NCC[91] based methods show a similar dominant perfusion defect in the anterior segment (arrow).

between the perfusion parameters obtained from ground truth and FT contours. Since the MPRI depends on stress and rest up-slopes, it is not surprising that the MPRI values also show a good correlation between the ground truth and the proposed method (R^2 = 0.98). In the Bland Altman plot (Figure 4.8), the distribution around the mean suggests the absence of both a systematic error and a visible trend for the proposed method.

4.5.3 Clinical significance

An example demonstrating the diagnostic accuracy of the proposed method is provided in Figure 4.10, which shows the distribution of the mean of myocardial intensities across the complete sequences in different slices. Higher intensities in the myocardium show normal perfusion whereas the low intensity areas indicate hypo-perfused regions. The corresponding slices of both ground truth (first row) and the registered sequences (FT) show that if used for diagnosis, the registered images will result in the same interpretation, i.e., low perfusion in mid and basal inferolateral segments.

A comparison of the ground truth with other methods (Figure 4.11) based on myocardial blood flow[111] yields similar observations. Although only basal slice related results are shown due to space constraints, they serve to illustrate the differences or similarities in the diagnostic inferences a clinician would make from these images. The image corresponding to the proposed method corroborates the findings in the ground truth image i.e., the reduction of blood flow in inferolateral segment. However, the images corresponding to ICA[154] and NCC[91] based methods, show a dominant perfusion defect in the anterior segment. It is evident that the cranio-caudal motion was not corrected by these methods as a higher blood flow is shown in the inferior segments in Figure 4.11 (c) and (d), which implies the incursion of blood pool in the myocardium. In contrast, Figure 4.11 (b) shows low blood flow similar to that shown in Figure 4.11 (a), which suggests that the proposed method does well to avoid the incursions of pixels from LV blood pool into the myocardium.

4.5.4 Limitations

The proposed approach also has a number of limitations. In particular, when faced with sequences that include one or more frames containing a significant variation in myocardial shape and size, the performance of the algorithm is sometimes unpredictable (outliers in Figure 4.4), which is not surprising given that the underlying model applies only 2D translations based on the assumptions that the cardiac motion and through plane movements are absent. To compensate for the deformations and through plane motion, non-rigid transformations can be included. However, it has been shown that the correction of deformations using non-rigid registration only slightly improves the motion compensation when compared to rigid registration[267]. The absence of through plane motion correction in the proposed algorithm is therefore not a significantly limiting factor.

Another limitation of this method is its susceptibility to the intensity changes in the organs surrounding the heart. This is dealt with to some extent by automatically selecting an ROI, which tends to force the estimation to be performed only within a region containing the RV and the LV. However, the precise selection of this ROI cannot always be guaranteed with the current implementation. Future work will therefore focus on a more robust automatic detection of the ROI.

4.6 Conclusion

We presented a novel registration method that eliminates large motion artifacts, especially present in stress CMRP images of patients with suspected CAD. The proposed method (FT) was validated on 120 sequences consisting of rest and stress datasets from 20 patients prone to CAD and outperformed ICA[154] and NCC[91] based existing implementations. Particularly encouraging were the mean registration errors of less than a pixel, and the agreement between the perfusion parameters obtained from the ground truth and the FT registered sequences. With fast processing time, robustness to large displacements, and high clinically accuracy, the proposed method is a promising step towards the near-automated perfusion quantification in CMRP images.

Acknowledgments

We are grateful to Dr. Rob van der Geest for his suggestions on the computation of perfusion parameters and to Ms. Hortense Kirisli for her contributions related to data processing.